**Journal of Korean Powder Metallurgy Institute**
Vol. 9, No. 4, 2002

P M 리 뷰

# A New PIM Joining Process

**Hideshi Miura**
*Graduate School of Science and Technology, Kumamoto University*
*2-39-1 Kurokami, Kumamoto 860-8555, Japan*
(Received July 30, 2002 ; Accepted form August 14, 2002)

**Abstract** A new PIM in-process joining technique has been developed for more complicated and functional PIM components by application of the exuded wax from the green compacts during solvent debinding step. At first, various stainless steels and iron compacts with rectangular shape were combined, and the joining behaviors and properties were investigated by shear and tensile test, and microscopic observation. Subsequently, perfect joined three pieces of thin and hollow compacts were obtained for the combination of same and different stainless steels, and it was difficult to join the iron and stainless steel compacts in hydrogen atmosphere because of the different starting temperature of shrinkage. However, pretty good joined iron and stainless steel compacts were obtained by consideration of particle size and vacuum atmosphere. Finally, for the combination of ferro-silicon and austenitic stainless steel compacts, high functionality (magnetic (1.60Tesla) & non-magnetic) and perfect joint were obtained.

**Keywords :** Powder injection molding, In-process joining, Solvent debinding, Iron and stainless steel, Multi-functionality.

## 1. Introduction

Powder injection molding(PIM) process is now well-known to be an advanced powder processing technique for near net shaping of high density, high performance and complicated parts. However, there still remains the issue of limitation in the shape because of using the die. Application of the joining technique may be one of approaches to solve the above problems.[1-3)]

In this study, a new joining technique has been developed by using effectively the exuded wax from the green compacts during solvent debinding to produce more complicated and functional components such as the combination of non-magnetic (SUS304 L, 316 L) and magnetic (SUS420J1, Fe, Fe-3Si) materials. This paper describes mainly the influence of the debinding conditions, the combination of joining materials, and the sintering atmospheres on the joining behavior, strength and microstructures of the joined compacts.

## 2. Experimental Procedure

The powders used in this study were gas atomized

**Table 1. Chemical compositions of the powders used in this study.**

| Powder | Particle size(μm) | Chemical composition (mass%) | | | | | | | | |
|---|---|---|---|---|---|---|---|---|---|---|
| | | Cr | Ni | Mo | Si | Mn | C | N | O | Fe |
| SUS304L | 11.5 | 19.6 | 11.9 | - | 0.6 | 0.1 | 0.02 | - | 0.07 | bal. |
| SUS420J1 | 13.2 | 12.7 | - | - | 0.4 | 0.1 | 0.19 | - | 0.07 | bal. |
| SUS316L | 4.2 | 16.5 | 12.5 | 2.1 | 0.8 | 0.8 | 0.03 | - | - | bal. |
| | 9.6 | 16.8 | 12.5 | 2.1 | 0.8 | 0.8 | 0.03 | - | - | bal. |
| Carbonyl Fe | 4.9 | - | - | - | - | - | 0.01 | 0.17 | <0.01 | bal. |
| | 10.2 | - | - | - | - | - | 0.07 | <0.01 | 0.34 | bal. |

stainless steel powders such as SUS420J1(mean particle size(m.p.s.) : 13.2 μm), SUS304 L(m.p.s. : 11.5 μm) and SUS316 L (m.p.s. : 4.2 μm and 9.6 μm). And also carbonyl iron powders(m.p.s. : 4.9 μm and 10.2 μm) were used. The chemical compositions of those powders are shown in Table 1. Those powders were admixed with the binder composed 69mass% paraffin wax, 10mass% carnauba wax, 20mass% polypropylene, and 1mass% stearic acid at 423 K for 3.6 ks. The powder loading in those mixtures was about 60 vol%. The mixtures were injection molded with a reciprocating screw machine into rectangular, and thin and hollow compacts. The green compacts were coupled as shown in Figure 1 and 2. For the debinding, extraction debinding by condensed solvent, which was conducted at 358 K for 18 ks in n-heptane, was used to partially remove the wax. At that time, the fused and exuded wax from the green compacts was applied in joining the couples. Following this treatment, final thermal debinding was performed by covering the green compact on the porous $Al_2O_3$ substrate with fine $Al_2O_3$ powder, and heating at 0.067 K/s to 873 K, followed by sintering at 1573 K for 3.6 ks in hydrogen gas or vacuum. The joining strength and microstructure were investigated by shear and tensile test, and photomicroscopic analysis, respectively.

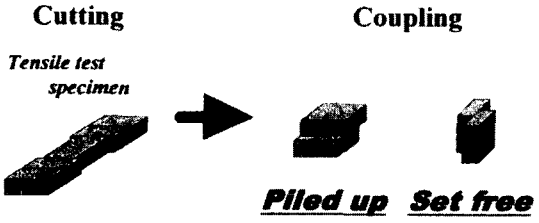


**Fig. 1. Schematic illustration of the coupling for rectangular compacts.**

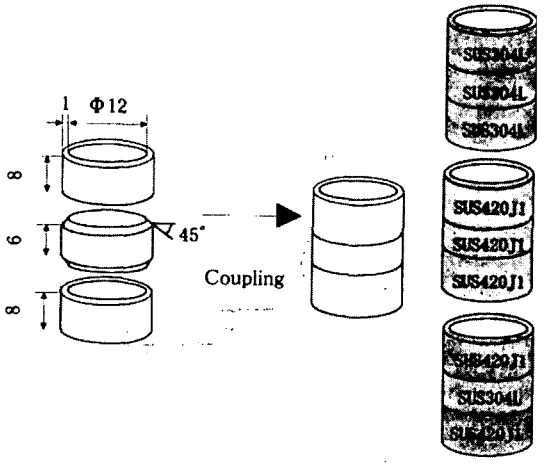


**Fig. 2. Schematic illustration of the coupling for thin and hollow compacts.**

## 3. Results and Discussion

### 3.1. Optimization of solvent debinding conditions

At first, the influence of solvent debinding temperature on the shape retention was investigated by using Fe/Fe couple mounted as shown in Figure 3(A). Figure 4 shows the aspect of the solvent debound couples at

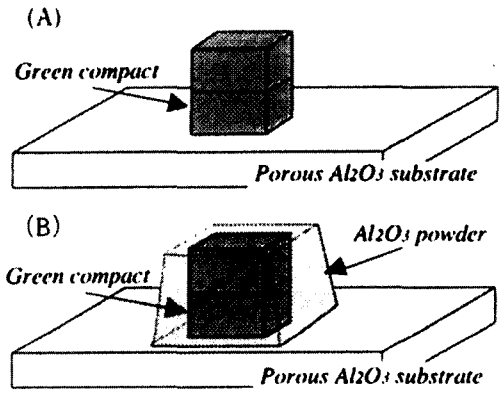


**Fig. 3. Schematic illustration of placing the couple in solvent debinding.**

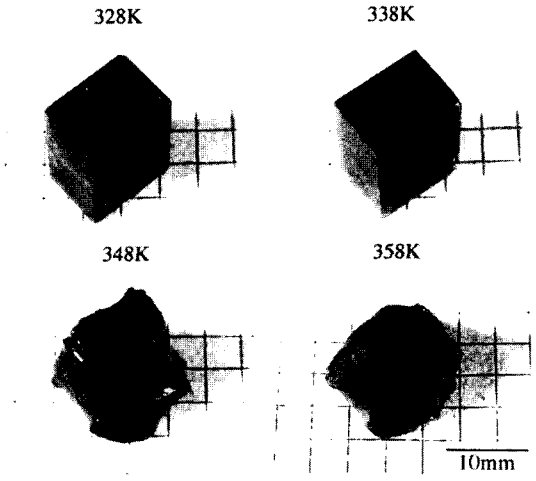


**Fig. 4. Aspect of the solvent debound Fe/Fe couples at 328, 338, 348 and 358 K.**

328 to 358 K. Clearly, the deformation is increased with an increase in temperature. The solvent debound couples at low temperatures(328 and 338 K) show good shape retention, but the binder removal contents are not so high as shown in Figure 5. This makes it difficult to join the couples by sintering as noted later on. Thus, the sound debound and sintered couples were not obtained by using Fe/Fe couple mounted as shown in Figure 3(A). On the other hand, Fe/Fe couple covered with fine $Al_2O_3$ powder (Figure 3(B)) showed good shape retention even at high solvent debinding temperature of 358 K as shown in Figure 6, and the binder removal was as high as 70% due to the wicking effect. Therefore, covering the green compacts with fine $Al_2O_3$ powder during solvent debinding was adopted in subsequent experiments.

Figure 7 shows the aspect of fractured surface from the joining interface for Fe/Fe couples, solvent debound at various temperatures. The specimen debound at 328 K shows smoothed surface which means not so strong joining. On the other hand, the specimens debound at over 338K show roughened surfaces which means strong joining, and looks like one piece. Thus, the optimum solvent debinding temperature was seemed to be 358 K.

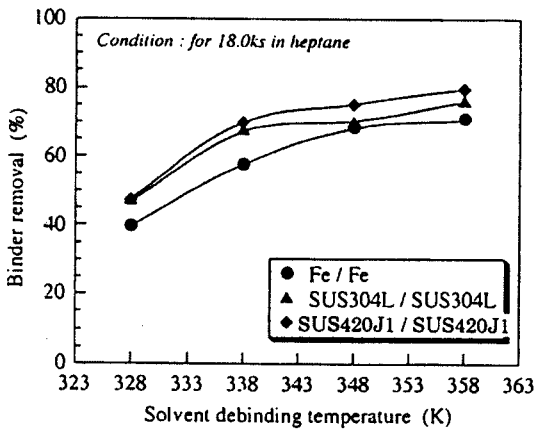


**Fig. 5. Effect of the solvent debinding temperature on the binder removal.**

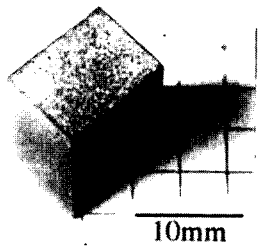


**Fig. 6. Aspect of the solvent debound Fe/Fe couple covered with $Al_2O_3$ powder at 358 K.**

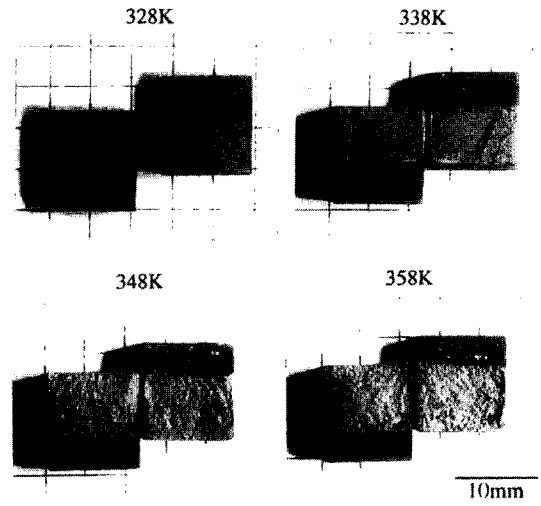


**Fig. 7. Aspect of the fracture surfaces for Fe/Fe couples, solvent debound at various temperatures.**

### 3.2. Joining properties for the couples of same materials

Figure 8 shows the effect of solvent debinding temperature on the shear strength for the couples of same materials (Fe/Fe, SUS304L/SUS304L, SUS420J1/SUS 420J1) sintered at 1573 K for 3.6ks in $H_2$. Sintered densities of all compacts were about 96% of theoretical.

Shear strengths of all couples increase with increasing temperature, and the strength of each couple debound at high temperature is similar to essential strength of the injection molded compact sintered under the same conditions.

Figure 9 shows the microstructure of the sintered and joined area for each couple debound at 328 and 358 K. In every couples debound at low temperature of 328 K non-joined part due to the substantial amount of retained binder are observed, which cause a low shear strength and the large scattering. On the other hand, all the couples debound at high temperature of 358 K show the perfect joints, that is, the traces of original joined interfaces are not observed. This leads the high shear strength. Moreover, there was not difference between the strength and microstructure of the piled up compact and that of the set free compact as shown in Figure 1.[3)]

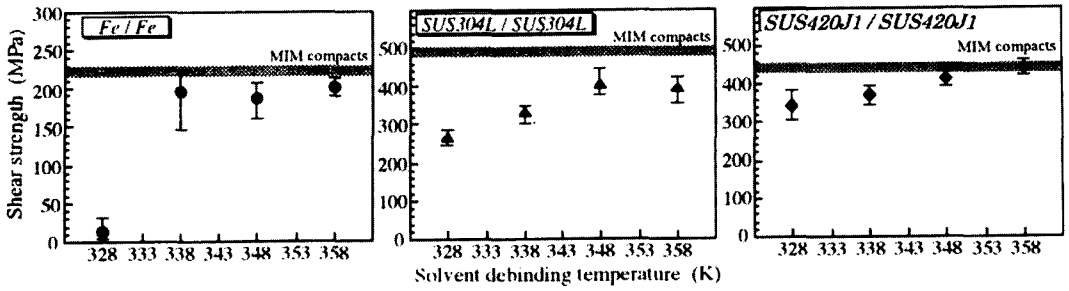


**Fig. 8. Effect of the solvent debinding temperature on the shear strength for the couples of same materials sintered at 1573 K.**

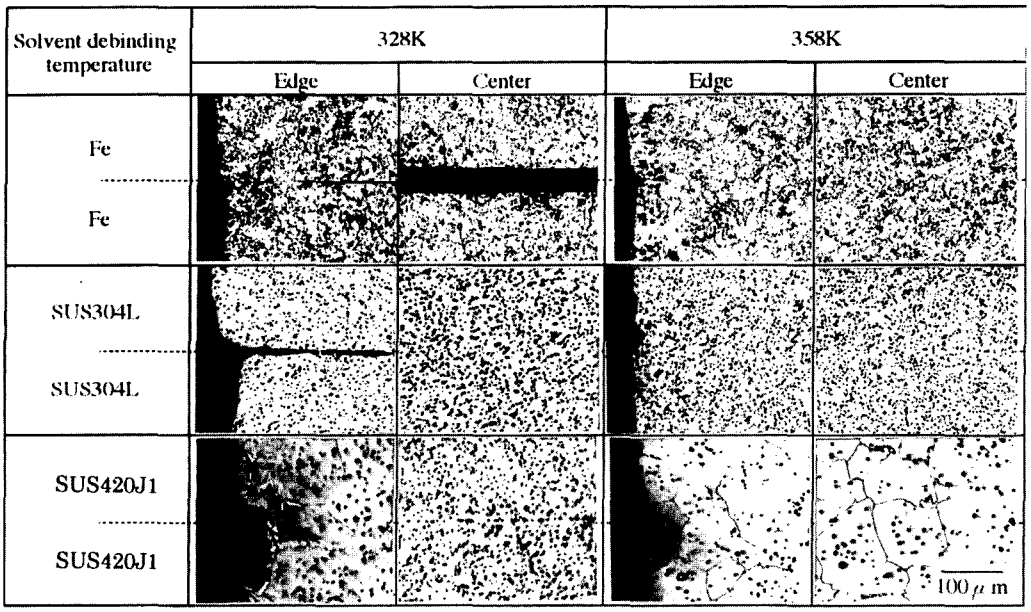


**Fig. 9. Microstructures of the joined area for the couples of same materials sintered at 1573 K.**

### 3.3. Joining properties for the couples of different materials

Figure 10 shows the effect of solvent dibinding temperature on the shear strength of SUS304L/SUS420J1 couples sintered at 1573 K for 3.6 ks in $H_2$. In this case too, the strength increases with increasing temperature. Figure 11 shows the microstructure of the perfect joined area, but the fracture occurs at the side of SUS420J1. This seems to be caused by the changing from the martensitic to the ferritic structure of SUS420J1 due to the decarburization (0.19→0.03 mass%C) under the reducing atmosphere($H_2$). Moreover, a new reacted layer due to the diffusion of Ni element is formed at the side of SUS420J1 and the

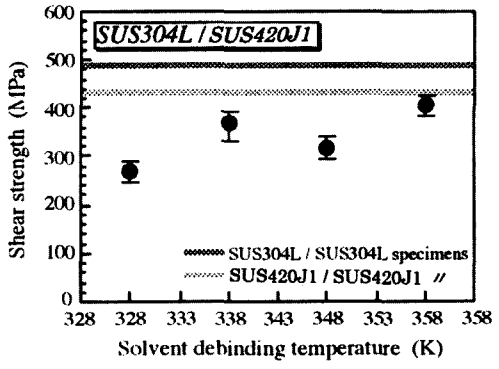


**Fig. 10. Effect of the solvent debinding temperature on the shear strength of SUS304L/ SUS420J1 couples.**

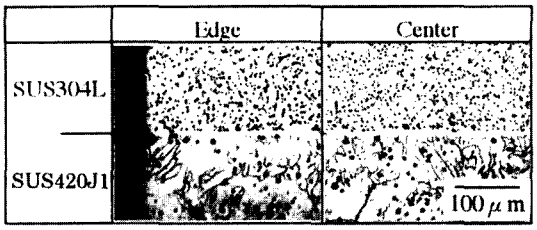


**Fig. 11. Microstructures of the joined area for SUS304L/SUS420J1 couple.**

crack propagates exactly between the reacted layer and the ferritic structure. This also reflects the high joining strength.

### 3.4. Joining of the thin and hollow compacts

Figure 2 shows schematically an example of the coupling the same and different materials. Three pieces of thin and hollow compacts were injection molded individually and mounted fitly. However, it was very difficult to obtain the perfect joining by only mounting. Therefore, porous alumina substrate with the holes were prepared, and the specimen was put into the hole and embeded the alumina powder into the inside of specimen, and then final thermal debinding and sintering were performed. From this procedure sound joined specimens were obtained as shown in Figure 12, not only for the combination of same materials, but also for the combination of different materials.[4] Figure 13 shows the microstructures of the perfect joined area for each combined specimens, that is, the traces of original joined interfaces are not observed except the couple of different materials. Figure 14 shows the tensile strength of the joined specimens and bulk compacts. The joined specimens (SUS420J1/420J1, SUS304L/304L) show almost the same strength as the bulk compacts(MIM SUS420J1, MIM SUS304L). For the tensile testing of different materials (SUS420J1/304L), fracture occured at the side of SUS304L. Because the strength

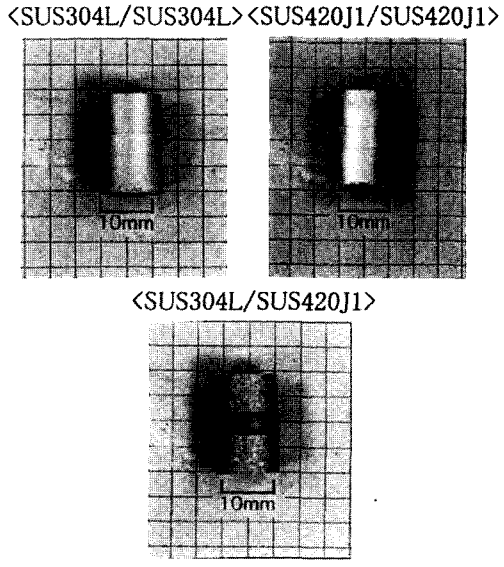


**Fig. 12. Aspects of the joined compacts by mounting in hole of $Al_2O_3$ substrate.**

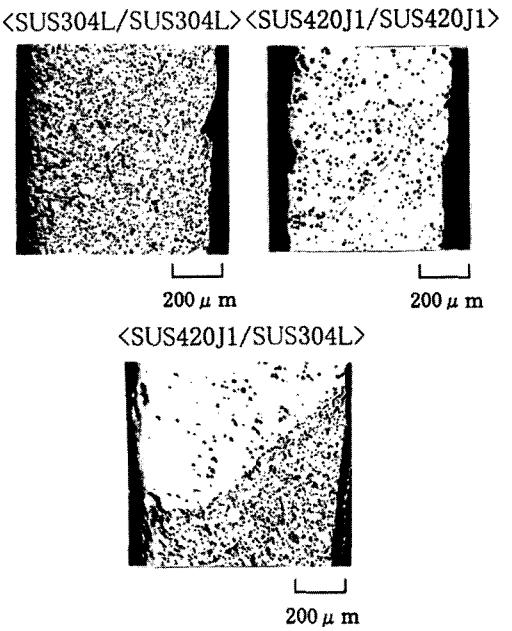


**Fig. 13. Microstructures of the joined area for various couples, sintered at 1573 K for 3.6 ks in $H_2$.**

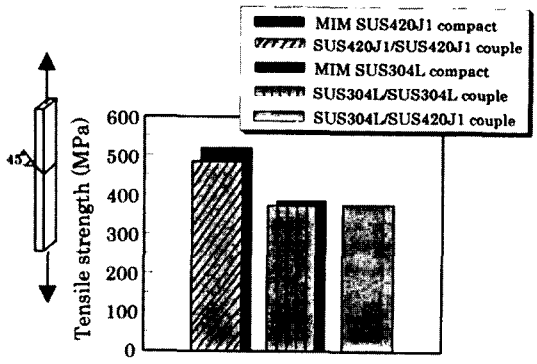


**Fig. 14. Tensile strength of various couples and MIM compacts, sintered at 1573 K for 3.6 ks in $H_2$.**

of SUS304L is essentially lower than that of SUS 420J1. Therefore, the strength of joined different materials was very similar to that of the joined SUS304L compacts.

By the way, pure iron is preffered industrially as a strong soft-magnetic material. So subsequently, the joining of pure iron and austenitic stainless steel(SUS 316L) compacts was investigated for more functional material with magnetic and non-magnetic properties. However, sintering behavior such as starting temperature of shrinkage is considerably different between both powders. Therefore, the both powders with different particle size were prepared to adjust the densification behavior. The chemical composition of two types of carbonyl iron powders with mean particle sizes of about 5 and 10 μm, and also the chemical compositions of austenitic stainless steel(SUS316L) powders with particle size of about 4 and 10 μm are shown in Table 1. For the combination of stainless steel powder with about 10 μm particle size and both iron powders with 5 and 10 μm particle sizes, there was not joined area by using hydrogen atmosphere as shown in Figure 15. Even for the combination of stainless steel powder with 4 μm particle size and iron powders, there was a slight joint only at the center of the combination of SUS316L(4.2 μm) and Fe(10.2 μm).

Figure 16 shows the scaning electron microanalysis images of the interface of iron and stainless steel compacts sintered at 1173 K for 60 s in $H_2$. For the iron side, it was obviously observed that the sintering was already started. On the other hand, there remained original powder shape in the stainless steel side. Figure 17 shows the shrinkage of four different powder compacts at various temperatures in hydrogen atmosphere. Obviously, both iron powder compacts start the sintering at low temperature as compared to both stainless steel powder compacts. Namely, a kind of crevice or crack was formed at the interface because of different sintering shrinkage.

By the way, vacuum is usually used for sintering the stainless steel compacts. Therefore, we tried to join the same couples in vacuum atmosphere. It was still difficult to obtain the good joined area, especially for the stainless steel powder with large particle size. On the other hand, nearly perfect joint were obtained by using both powders with fine particle sizes as shown in Figure 18. Figure 19 shows the shrinkage of four powder compacts in vacuum atmosphere. The shrinkage curve of stainless steel powder with fine particle size shifted a little bit to low temperature as compared to the shrinkage curve in hydrogen atmosphere(Figure18). However, it was difficult to obtain high magnetic flux

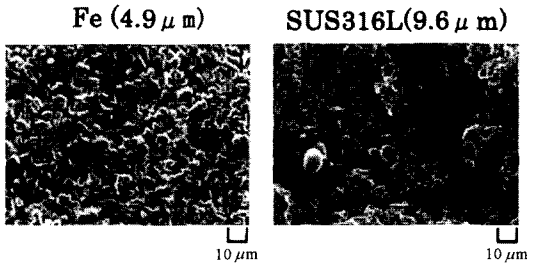


**Fig. 16. SEM images of the interface for Fe/SUS316L couple sintered at 1173 K for 60 s in $H_2$.**

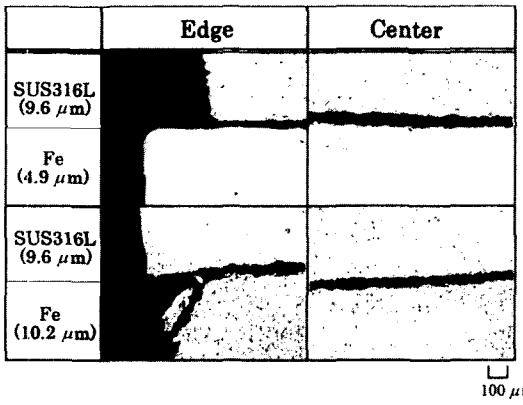


**Fig. 15. Microstructures of the joined area for Fe/SUS316L(9.6 μm) couples, sintered at 1573 K for 3.6 ks in $H_2$.**

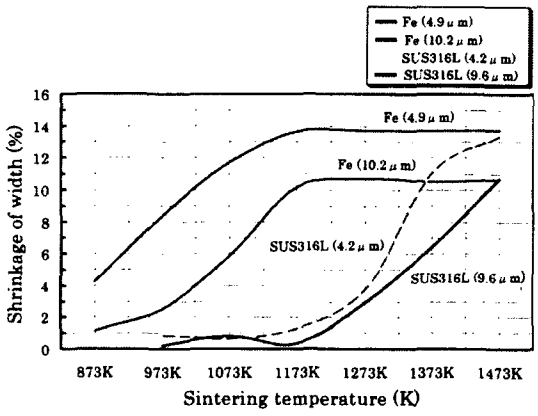


**Fig. 17. Effect of sintering temperature for 60 s in $H_2$ on the shrinkage of Fe and SUS316L compacts.**

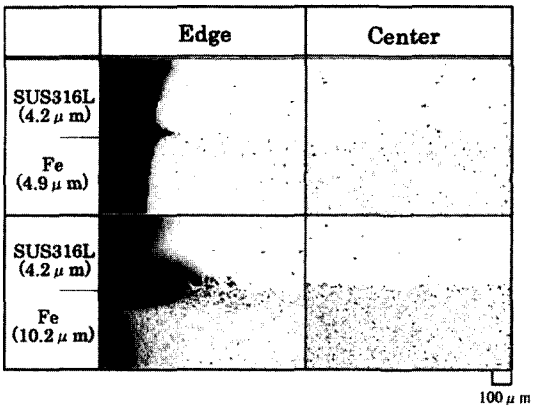


**Fig. 18. Microstructures of the joined area for Fe/SUS316L couples sintered at 1573 K for 3.6 ks in vacuum.**

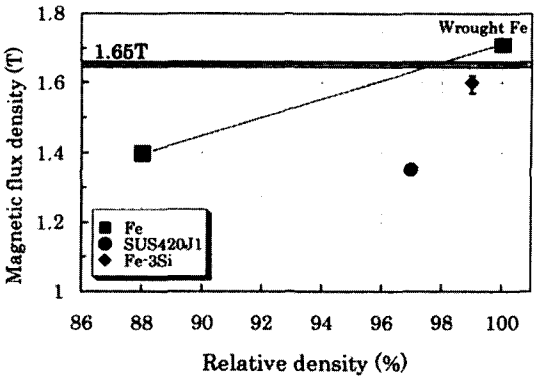


**Fig. 20. Effect of relative density on the magnetic flux densities of various compacts sintered at 1573 K for 3.6 ks in $H_2$.**

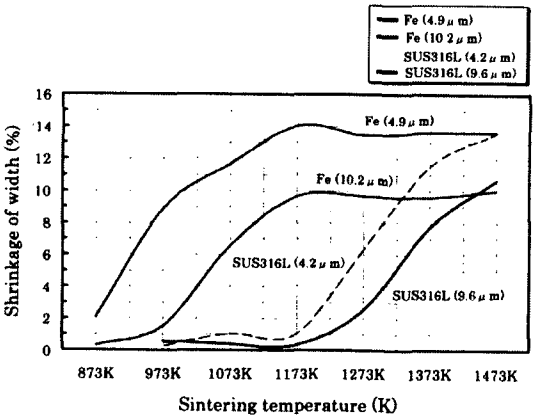


**Fig. 19. Effect of sintering temperature for 60 s in vacuum on the shrinkage of Fe and SUS316L compacts.**

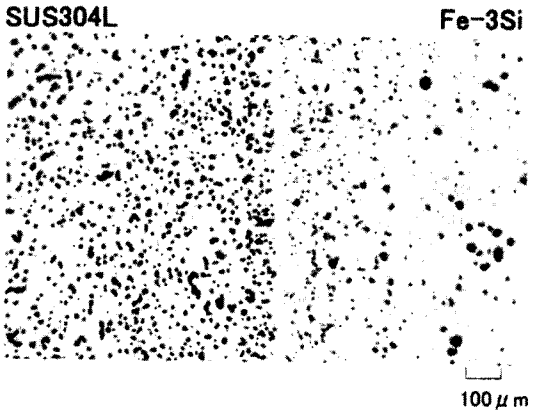


**Fig. 21. Microstructure of SUS304L/Fe-3Si couple sintered at 1573 K for 3.6 ks in $H_2$.**

density by using iron powder. Our magnetic target was 1.65Tesla. So we tried to use ferrosilicon powder as magnetic material. Almost the high magnetic flux density near to the target was obtained as shown in Figure 20. Figure 21 shows the perfect joint of stainless steel and ferrosilicon powder compact by a new PIM In-process joining technique.

## 4. Conclution

In order to develop a new PIM in-process joining for more complicated shape and more functional components, the exuded wax from the green compact during solvent debinding step has been applied to join the couple of same or different materials(iron and stainless steel). The results obtained are summarized as follows:

1) The deformation during solvent debinding followed by thermal debinding was prevented from covering the couple of green compacts with $Al_2O_3$ powder. As the solvent dibinding temperature increased, the binder removal content was increased by the wicking effect and a good adhesive joined couple was obtained.

2) Perfect joined couples of the same (SUS304L/SUS304L, SUS420J1/SUS420J1) and different (SUS 304L/SUS420J1) materials were obtained by PIM in-process joining.

3) For the couple of iron and stainless steel compacts, joining was difficult because of the different starting temperature of shrinkage. However, excellent joining was obtained by using stainless steel powder with fine particle size and vacuum sintering.

4) For the couple of austenitic stainless steel(SUS 304L) and ferro-silicon compact, high functionality (magnetic(1.60Tesla) & non- magnetic) and perfect joint were obtained.

## References

1. H. Miura, K. Hazama, K. Baba, and T. Honda: J. Japan Soc. Powder and Powder Metal., **44** (1997) 437.
2. H. Miura and K. Mori: Proc. of the 1998 Powder Metal lurgy World Congress & Exhibition, EPMA, **3** (1998) 51
3. H. Miura and K. Mori: J. Japan Soc. Powder and Pow der Metal., **46** (1999) 927.
4. H. Miura, T. Yano, and M. Matsuda: J. Japan Soc. Pow der and Powder Metal., **48** (2001) 1097.